Forward physics results from ATLAS

Gareth John Ashley Brown
On behalf of the ATLAS Collaboration

School of Physics & Astronomy, University of Manchester, Oxford Road. Manchester M13 9PL. U.K.

The rapidity gap cross section and the dijet with jet veto analyses that were measured at the ATLAS experiment at the LHC are discussed. The rapidity gap cross section analysis measures the differential cross section as a function of the forward rapidity gap size. This diffractive cross section is compared to PYTHIA 8, PYTHIA 6 and PHOJET. The measured diffractive cross section is approximately 1mb per forward rapidity gap size for a gap size greater than 3. The dijet with jet veto analysis measures the fraction of dijet events that remain after the application of a jet veto of 20 GeV in the rapidity region between the dijet system. This fraction is presented against the rapidity separation of the boundary dijets (in the range $0 < \Delta y < 6$) and the average transverse momentum of the boundary jets (in the range $50 < \bar{p_T} < 500$ GeV). The data are compared to a next-to-leading order plus parton shower prediction from the POWHEG-BOX and an all-order resummation using the HEJ calculation.

§1. Introduction

Two measurements from the ATLAS experiment at the LHC will be reported in these proceedings. The first study is the first ATLAS measurement of the inelastic cross-section as a function of the forward rapidity gap size. The rapidity gaps are destroyed by pile-up so data from low luminosity runs were used (giving an integrated luminosity of $7.1\mu b^{-1}$). The second study is a measurement of the jet activity in the rapidity region between a dijet system.

§2. Rapidity Gap Cross Sections in pp Interactions at $\sqrt{s} = 7\ TeV$

This section is based on the ATLAS conference note "Rapidity Gap Cross Section in pp Interactions at $\sqrt{s} = 7\ TeV$".[1] In this analysis the differential cross section is measured as a function of the forward rapidity gap size, which extends to the forward acceptance of the detector. A comparison of the data to different Monte Carlo (MC) generators' single diffractive dissociation (SD), double diffractive dissociation (DD) and non-diffractive (ND) contributions is shown.

The data used in this analysis were from the first LHC run in 2010. Only events for which the calorimeters and inner detecters were fully functional were considered. The MBTS trigger was used to collect events, and the integrated luminosity of the data used was 7.1 μb^{-1}. The run had a very low probability of pile-up (which could destroy the rapidity gap) and suspected pile-up events were removed.

Both the ATLAS[2] calorimeter and inner detector were used in this analysis. The ATLAS inner detector reconstructs charged particles with rapidity, $|\eta| < 2.5$. In this analysis only tracks with a transverse momentum,p_T, above 200 MeV are considered.

ATL-PHYS-PROC-2011-270
07 December 2011

The ATLAS calorimeter measures both electromagnetic (EM) and hadronic energy deposits out to $|\eta| < 4.9$. Calorimeter cell energy is determined to be significant by comparing the energy to the root-mean-squared electronic noise.

To help define the gap, the detector is split into 49 rings across the range $-4.9 < \eta < 4.9$. If there is neither a track with $p_T > 200MeV$ nor a significant cell energy, then the ring is classed as empty. A rapidity gap is formed by consecutive empty rapidity rings. A forward rapidity gap is the largest rapidity gap which extends to the forward acceptance of the detector. The MC generators, have the same rapidity rings, but they are defined as empty if there is no stable particle with $p_T > 200\ MeV$ in the ring. An additional floating gap (no requirement to be on edge of detector acceptance) is defined to optimise the ND, SD, and DD contributions of the MC generators. The floating gap has both a gap size, $\Delta\eta$, and a gap starting position, η_{start}. Fig. 1 shows the fraction of events in $\Delta\eta$ and η_{start} for both the data and one of the MC generators (PYTHIA 8[3]). The PYTHIA 8 distribution has the nominal mix of SD, DD and ND events, this is then optimised using a template to get better agreement to the data. Similarly, a template is created for the other MCs used for comparison, PYTHIA 6[4] and PHOJET.[5]

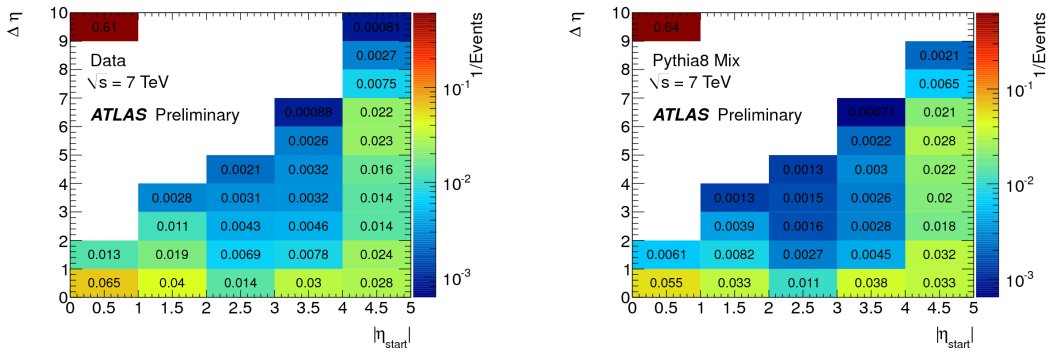

Fig. 1. Rapidity gap distribution is shown as a function of $\Delta\eta$ and η_{start} for both data (left) and PYTHIA 8 with the nominal mix of SD, DD and ND events (right).[1]

Fig. 2 shows the differential cross section as a function of the forward rapidity gap size, $\Delta\eta^F$ comparing the data to both PYTHIA 8 and PHOJET. In these plots, only $\Delta\eta^F > 2$ is shown, this cuts out the low $\Delta\eta^F$ which is dominated by the ND component. After $\Delta\eta^F = 3$ there is a plateau in the data. On the plateau, the diffractive cross section is $\sim 1mb \pm 0.2mb$ per rapidity gap size. At the plateau, the PHOJET curve agrees better with the data, while PYTHIA 8 has too high a differential cross section. While both PYTHIA 8 and PHOJET agree on the SD contribution, PYTHIA 8 has a significantly larger DD contribution.

§3. Dijet production with a jet veto

This section is based on the ATLAS paper "Measurement of dijet production with a veto on additional central jet activity in pp collisions at $\sqrt{s} = 7\ TeV$ using the ATLAS detector".[6] A jet veto was used to measure the fraction of dijet events

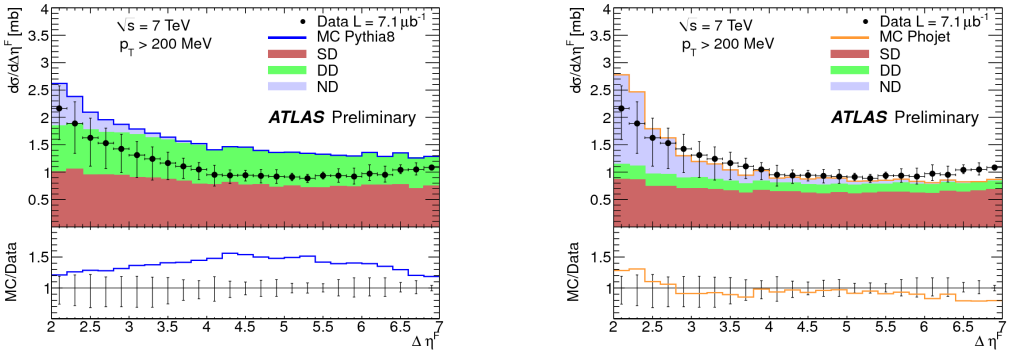

Fig. 2. Inelastic cross section as a function of the forward gap size for particles with $p_T > 200\ MeV$ and $\Delta\eta > 2$. The black points are the data with error bars which include both the systematic and statistical uncertainty. (Left) shows the data compared to PYTHIA 8 and (right) shows the data compared to PHOJET. Both show the breakdown of the different contributions to the differential cross section from SD, DD, and ND components from both generators.[1)]

without an additional jet with transverse momentum, p_T, greater than the jet veto scale, Q_0 (default value 20 GeV) in the dijets rapidity interval. Two boundary jets were defined as the two highest p_T jets in the event. They have average transverse momentum, $\bar{p_T}$, and rapidity separation, Δy. The boundary jets were required to have a $\bar{p_T} > 50\ GeV$ to be on the trigger plateau. The gap fraction is measured as a function of either Δy, or $\bar{p_T}$.

The jet algorithm used was the anti-k_t algorithm[7)] with a distance parameter R= 0.6 and with an input of calorimeter clusters. Only jets with $p_T > 20\ GeV$ and $|y| < 4.4$ were considered.

Only events where the detector was fully functioning and where there were stable beam conditions were used, and events were rejected if there were either badly measured jets, or jets arising from detector noise.

At large values of Δy or $\bar{p_T}$, fixed−order calculations are expected to fail, so leading order MC generators are not expected to agree well with the data. Resummation in either Δy or $\bar{p_T}$ is required, and so the data is compared to HEJ[8)] and the POWHEG-BOX.[9)] HEJ is a parton level event generator which supplies an all-order description of hard wide angle emissions. POWHEG-BOX supplies a NLO dijet calculation interfaced to the parton showering in PYTHIA[4)] and HERWIG.[10)]

The main systematic uncertainties come from the jet energy scale (JES)[11)] and the unfolding of the data. Both are weakly dependent on $\bar{p_T}$, but they both rise at large Δy. The JES increases with Δy as the jets occur in regions that have different JES uncertainties. The unfolding uncertainty rises as there are lower statistics in the large Δy region.

Fig. 3 (left) shows the gap fraction as a function of Δy for various $\bar{p_T}$ ranges. Fig. 3 (right) shows the ratio of the theory predictions to the data. HEJ agrees well with the data as a function of Δy for the low $\bar{p_T}$ slices, but gives too high a gap fraction at large $\bar{p_T}$. It is expected that HEJ would do well as a function of Δy, because the event generator's resumation is in Δy. POWHEG (with PYTHIA

parton showering) agrees well at low Δy for all $\bar{p_T}$ ranges, but gives too low a gap fraction for large Δy.

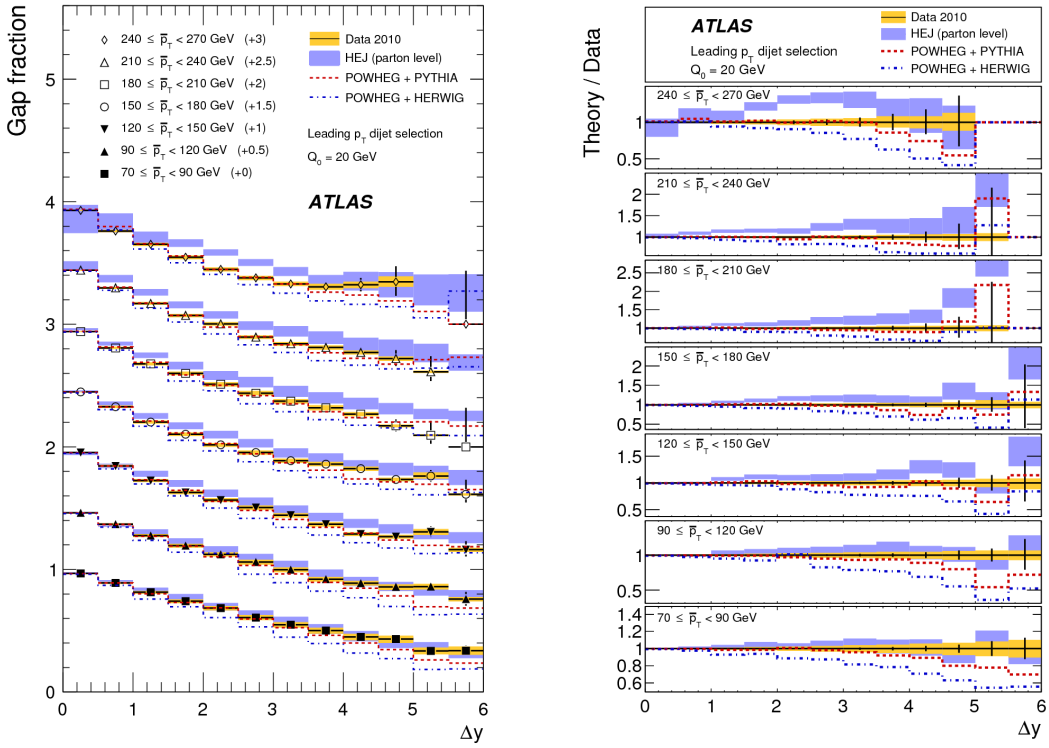

Fig. 3. Gap fraction as a function of the Δy for different $\bar{p_T}$ slices. (Left) Comparison of the data to both the HEJ and POWHEG predictions. (Right) The ratio of the HEJ and POWHEG predictions to the data.[6)]

References

1) ATLAS collaboration, *Rapidity gap cross sections in pp interactions at* $\sqrt{s} = 7TeV$, ATLAS-CONF-2011-059 (2011), https://cdsweb.cern.ch/record/1344487
2) ATLAS Collaboration, JINST **3** (2008), S08003
3) T. Sjostrand, S. Mrenna and P.Z. Skands, *Brief Introduction to PYTHIA 8.1*, Comput. Phys. Comm. **178** (2008), 852
4) T. Sjostrand, S. Mrenna and P.Z. Skands, *PYTHIA 6.4 physics and manual*, J. High Energy Phys. **05** (2006), 026, hep-ph/0603175.
5) R. Engel, Z. Phys. **C66** (1995), 203
6) ATLAS collaboration, *Measurement of dijet production with a veto on additional central jet activity in pp collisions at* $\sqrt{s}$*=7 TeV using the ATLAS detector*. J. High Energy Phys. **09** (2011), 053, CERN-PH-EP-2011-100; arXiv:1107.1641.
7) M. Cacciari, G.P. Salam and G. Soyez, *The anti-k_t jet clustering algorithm*, J. High Energy Phys. **04** (2008), 063, arXiv:0802.1189.
8) J.R. Andersen and J.M. Smillie, *High energy description of processes with multiple hard jets*, Nucl. Phys. Proc. Suppl. **205-206** (2010), 205, arXiv:1007.4449.
9) S. Alioli, P. Nason, C. Oleari, and E. Re, J. High Energy Phys. **06** (2010), 043, arXiv:1002.2581.
10) M. Bahr et al., Eur. Phys. J. C **58** (2008), 639, arXiv:0803.0883.
11) ATLAS collaboration, ATLAS-CONF-2011-032 (2011), https://cdsweb.cern.ch/record/1337782.